Increased N2O Production from Soil Organic Matter Following a Simulated Fall-Freeze-Thaw Cycle: Effects of Fall Urea Addition, Soil Moisture, and History of Manure Applications

Sisi Lin (slin4@ualberta.ca)
University of Alberta
Guillermo Hernandez-Ramirez
University of Alberta

Research Article

Keywords: priming effect, nitrous oxide, organic matter, denitrification, freeze, thaw.

Posted Date: May 25th, 2021

DOI: https://doi.org/10.21203/rs.3.rs-545397/v1

Increased N_2O production from soil organic matter following a simulated fall-freeze-thaw cycle: Effects of fall urea addition, soil moisture, and history of manure applications

Sisi Lin[1]; Guillermo Hernandez-Ramirez[1*]

1. Department of Renewable Resources, University of Alberta

* Corresponding author: Guillermo Hernandez Ramirez

Address:

426 Earth Sciences Building, Department of Renewable Resources Department, Faculty of Agricultural Life and Environmental Sciences, University of Alberta

Edmonton, AB, Canada T6G 2E3

E-mail: ghernand@ualberta.ca

Phone: +1-7804922428

17 **Abstract**

18 Adding nitrogen substrates to soils can induce short-term changes in soil organic matter (SOM)
19 transformations – a response termed the 'priming effect'. However, it is unknown how priming
20 effects on nitrous oxide (N_2O) emissions can be altered following a strong freeze-thaw cycle. A
21 mesocosm experiment evaluated two soil managements: with and without history of manure
22 applications. These soils were subjected to three moisture regimes: Low, Medium and High.
23 Apart from the controls, which received no N, we banded ^{15}N-labelled urea into these soils
24 representing a typical fall fertilization, and subsequently simulated a wide fall-freeze-thaw cycle,
25 with temperatures from +2, to -18, and finally +23°C, respectively. The overall highest N_2O
26 production was observed 1 day after thawing. At that time, measurements of N_2O site preference
27 indicated that denitrification produced 83% of the N_2O flux. Relative to the unamended controls
28 (baseline), adding urea consistently triggered a 24% greater cumulative N_2O production
29 specifically originated from SOM following thawing (245 vs. 305 μg N_2O-N kg^{-1} soil, P= 0.022).
30 This substantiates a positive priming of SOM that manifested shortly after the rapid, wet thawing
31 of the soils. Soils having a manure history or higher moisture also exhibited an augmented
32 production of N_2O from SOM (Ps< 0.01). Although the overall priming of SOM was positive,
33 two weeks after thawing, negative priming of daily N_2O fluxes also occurred, but only in soils
34 under High moisture. Besides urea additions, the propensity for primed N_2O emissions from
35 SOM after thawing was influenced by increasing moisture and earlier manure applications.

36 **Key words:** priming effect, nitrous oxide, organic matter, denitrification, freeze, thaw.

1. Introduction

Nitrous oxide (N_2O) is a potent greenhouse gas – with even 300-fold higher global warming potential than carbon dioxide (CO_2) on mass basis (Parry et al. 2007, Intergovernmental Panel on Climate Change 2013). More than half of the anthropogenic sources of N_2O are linked to agricultural landscapes (Parry et al. 2007, Intergovernmental Panel on Climate Change 2013, Chai et al. 2020), where manure and synthetic N fertilizers are recurrently applied (Lin et al. 2017, Grant et al. 2020, Thilakarathna et al. 2020). Such N additions not only provide substrates for N_2O emissions directly, but they can also stimulate mineralization of pre-existing SOM, which would subsequently lead to additional N_2O emissions indirectly – a response termed the 'priming effect' (Thilakarathna and Hernandez-Ramirez 2021). In other words, in the case of N_2O emissions from soils, priming consists of the fertilizer-induced N_2O emissions that originate from SOM mineralization. In further details, the magnitude and direction of N_2O priming is a function of the short-term acceleration (positive priming effect) or retardation (negative priming effect) of SOM-derived N_2O emissions from a soil receiving N compared to an unamended control as baseline. A comprehensive understanding of N_2O priming effects can improve quantification, proactive mitigation and ability to predict N_2O emissions from agricultural soils (Grant et al. 2020).

As climate change continues to take place, extreme fluctuations in the weather conditions can occur with increased frequency. Although soil freezing and thawing are already common phenomena in cold regions with relatively high latitude and altitude, the intensity and frequency of freeze-thaw cycles are gradually increasing as a feedback to escalating climate change

(Goldberg et al. 2008, Easterling et al. 2017). This applies to large temperate regions located in North America and Eurasia where annual croplands typically dominate the landscape. Within this context, earlier laboratory and field studies have examined N_2O emissions taking place over freeze-thaw cycles (Wagner-Riddle et al. 2007, Goldberg et al. 2008, Wolf et al. 2010, Wu et al. 2010, Yanai et al. 2011, Abalos et al. 2016). These reports indicate that N_2O fluxes during spring thaw can typically account for 30-90% of the annual N_2O emissions. A recent field study in western Canada found that at least 67% of the annual N_2O emissions occurred during the spring thaw in soils that had received liquid manure in the previous fall (Lin et al. 2017, Grant et al. 2020). Soil thawing activates N_2O production not only because of fast increases in ambient temperature but also because of sudden increases in soil water content caused by snow and ice melting (Wolf et al. 2010, Thilakarathna et al. 2020). It has been documented that increased moisture influences N_2O production by displacing and reducing oxygen availability, which drives a shift towards microbial utilization of nitrate as terminal electron acceptor during denitrification (Davidson 1991, Ruser et al. 2006, Lin and Hernandez-Ramirez 2020). Nevertheless, there is currently a paucity of knowledge on how freeze-thawing can influence the production of N_2O from SOM and the associated priming effects caused by labile N additions.

In addition to examining the priming of SOM, there is also a growing interest to assess the underlying processes of N_2O production. Both nitrification and denitrification contribute to N_2O fluxes from soils (Butterbach-Bahl et al. 2013). However, it is still unclear which of these processes is dominant during peak N_2O emissions in manured soils (Lin et al. 2017, Thilakarathna et al. 2020). As aforementioned an accelerated biological activity immediately

following thawing can critically deplete O_2 concentrations in the soil microsites, and hence it is hypothesized that the contribution of bacterial denitrification to N_2O production would also increase (Yanai et al. 2011). The ^{15}N isotope ratios at the central (α; ^{14}N-^{15}N-O) and terminal (β; ^{15}N-^{14}N-O) positions within the N_2O molecule – known as site preference (SP) – can reveal the dominant process contributing to N_2O production (Toyoda and Yoshida 1999, Toyoda et al. 2011, Yamamoto et al. 2017). The difference between α and β can be expressed as SP= $\delta^{15}N^{\alpha}$ - $\delta^{15}N^{\beta}$ (Toyoda and Yoshida 1999, Yamamoto et al. 2017). When N_2O fluxes become sufficiently large, this SP analytical approach enables us to examine and apportion the major N_2O producing pathways (i.e., nitrification vs. bacterial denitrification) (Zimmerman et al. 2011, Daly and Hernandez-Ramirez 2020, Thilakarathna and Hernandez-Ramirez 2021).

To address the abovementioned unknowns, we conducted a mesocosm experiment with the aim of investigating N_2O fluxes and sources (i.e., urea-N versus SOM-N) under increasing soil moisture regimes over a simulated fall season that included a urea addition followed by a strong freeze-thaw cycle in soils that had experienced contrasting histories of manure management. More specifically, this study focused on the dynamics of the N_2O priming effects caused by fall-added urea shortly after a sudden thawing. The following hypotheses were tested: i) compared with soils without urea addition (control baseline), adding urea would trigger a positive priming effect of N_2O emissions derived from SOM-N; ii) larger priming of N_2O production from SOM-N would occur in soils that had previously received recurrent manure applications; iii) increasing soil moisture would amplify SOM-derived N_2O production.

2. Materials and Methods

2.1 Soil collection

Soils (0-15 cm depth) were collected from experimental plots receiving spring manure (SW) and without a history of liquid manure injections (field control, CT). The soil was collected in October 2016 from a site located at the Edmonton Research Farm (53°29'30''N, 113°31'53''W), Alberta, Canada. The experimental site and field management have been described in Lin et al. (2017). The physical and chemical properties of the soils are shown in Table 1. Field moist soils were mixed and passed through an 8-mm sieve to homogenize and remove any large fragments and plant residue. After mixing, subsamples were oven-dried (105 °C) for 24 hours to measure the water content. Soils were stored at 2 °C until establishing the experiment.

2.2 Experimental setup

The experiment consisted of four sequential phases: i) an initial pre-conditioning phase, ii) a fall phase including urea addition, iii) a freezing phase, and iv) thawing phase.

The experiment was established in 5.5-L plastic pots 21 cm in height and 19.8 cm in inner diameter at the top of the container. In each pot, 5.5 kg of soil (as oven-dry equivalent) were packed in increments up to 5.0 L (18.4 cm height) to a bulk density of 1.1 g cm^{-3}.

2.2.1 Pre-conditioning phase

To restore and resemble the soil condition as found in cropped fields, we conducted an initializing phase by growing wheat in all the pots in a greenhouse for 3 months. The air

118 temperature in the greenhouse averaged 23 °C (ranging from 12 to 36 °C). Twelve wheat seeds
119 (AC Muchmore, Canadian Western Red Spring cultivar) (FP Genetics, Regina, SK, Canada)
120 were planted to 4 cm soil depth in each pot in a circle about 1.5 cm from the pot edge. After
121 germination, the number of wheat plants was reduced to eight per pot. Soil moisture was kept at
122 57% water-filled pore space (WFPS) by weighting the pots and adding water every two days.

123 Once wheat reached tillering stage, all pots began receiving a 0.5 g L^{-1} of dissolved fertilizer
124 weekly (i.e., 20% N, 8% P_2O_5, 20% K_2O, 0.5% Mg, 0.02% B, 0.05% Cu, 0.4% Fe, 0.05% Mn,
125 0.005% Mo, 0.05% Zn and 2.8% ethylene diamine tetra-acetate as chelating agent). Throughout
126 the wheat growth period, each pot received an equivalent of 50.85 kg N ha^{-1} according to typical
127 fertilizer recommendations (McKenzie et al. 2013). The aboveground plant biomass (> 5 cm
128 height) was harvested and removed 3 months after seeding. To represent the crop residue, 5 g dry
129 matter of straw biomass was added to the soil surface of each pot. Two pots from each soil were
130 randomly selected for destructive soil sampling with the aim of measuring ammonium and
131 nitrate concentrations as well as ^{15}N isotopic composition in natural abundance. Six soil cores
132 were taken from each of the two selected pots with an auger (3.5 cm diameter and 18.4 cm
133 depth). The other pots were sealed with caps and stored at 2 °C until the beginning of the next
134 experimental phase.

135 **2.2.2 Treatment application and simulated fall phase**

136 Prior to applying the moisture and urea treatments, all pots were removed from 2 °C to room
137 temperature to facilitate air drying until reaching the target WFPS (e.g., 45%). For each of the

two soil managements (i.e., CT and SW), three moisture regimes and two N additions were applied as experimental treatments. The three soil moisture regimes were Low (i.e., WFPS of 45% over the fall, reaching 70% during freezing, and falling to 55% by the end of the thawing phase), Medium (i.e., 55-80-65% WFPS) and High (65-90-75% WFPS). The N addition treatments were urea (5 atom% ^{15}N) (Sigma-Aldrich, St. Louis, MO, US) and control (without urea addition). The experimental design was a factorial with three replicates. In sum, the three experimental factors were: history of field manure injection (i.e., CT and SW), three moisture regimes (Low, Medium and High), and N addition (urea and unamended control). A total of 36 experimental pots were used for flux measurement during the experiment.

The moisture and N addition treatments were established on Day 0 of the fall phase which lasted for 27 days. The N addition consisted of 0.29 g of powder consistency 5 atom% ^{15}N-urea per pot placed at 5 cm depth to represent fertilizer banding. This rate was equivalent to 85 kg N ha^{-1}, which simulates a common fall fertilization for a canola crop in the subsequent growing season. After applying the N treatment, room-temperature deionized (DI) water was added to achieve fall moisture levels of 45 (Low), 55 (Medium) and 65% (High) WFPS. As necessary, the WFPS was maintained by weighting the pots and adding DI water every day throughout the fall phase. All pots and glass flasks with DI water were kept at 2°C. Cardboard was placed 3-5 cm above the top of the pots to prevent rapid evaporation while still allowing air circulation.

2.2.3 Simulated freezing phase

On Day 28 after the beginning of the experiment, a freezing phase was started by moving all pots from a temperature of 2 to -18 °C. This freezing phase lasted for 27 days (i.e., Days 28 to 55 following the urea addition) which assured that the soil columns became completely frozen. Additionally, to simulate multiple water inputs that accumulate over a typical winter in Central Alberta (snow and ice precipitation), DI water (at 2 °C) was added during the freezing phase in three successive increments. These water additions were done incrementally in amounts equivalent to 8.3, 8.3 and 8.4% WFPS on Days 31, 37 and 45, respectively. Upon melting, this water input was calculated to increase the water content in the soil by a total of 25% WFPS, which is a typical increase from fall to early spring. For the Low moisture regime, this meant a change from 45 to 70% WFPS; for Medium moisture, from 55 to 80%; for High moisture, from 65 to 90%. In line with typical winter conditions, most of the water added over the frozen mesocosms solidified on the top of the soil surface and it remained frozen until the beginning of the succeeding thawing phase when it melted and infiltrated into the soil column.

2.2.4 Simulated thawing

On Day 56 after urea addition, all pots were moved from -18 °C to room temperature conditions to simulate a strong thawing. The room temperature averaged 23 °C, ranging from 20.4 to 25.9 °C as recorded with a HOBO UX100-001 data logger at 1 Hz (Onset® Computer Corporation, Bourne, MA, USA). After the rapid soil thawing on Day 56, soil moisture content was allowed to gradually decrease by 0.5% WFPS daily. The total moisture decrease was 15% WFPS evenly

distributed over 30 days (from Day 56 to 86 after the urea addition). Soil moisture content was monitored and adjusted daily by weighting the pots and adding room temperature DI water as necessary. On the last day of the experiment (Day 86), three soil cores were taken from each pot with an auger (3.5 cm diameter and 18.4 cm depth). These composite soil samples enabled us to determine ammonium and nitrate concentrations as well as ^{15}N isotopic composition.

2.3 Measurements of N_2O fluxes and isotopic composition

The mixing ratios of ^{14}N-^{14}N-^{16}O, ^{14}N-^{15}N-^{16}O (α) and ^{15}N-^{14}N-^{16}O (β) (Ostrom et al. 2021) were quantified in a continuous mode via direct absorption spectroscopy at wavenumber of 2188 cm^{-1}. Briefly, the analyzer was an Aerodyne (Aerodyne Research, Inc., Billerica, MA, USA) with a thermoelectrically-cooled, mid-infrared quantum cascade laser, equipped with 200-m path length analytical cell (2 L volume at 30 Torr vacuum), and Nafion tubing (Perma Pure, Lakewood, New Jersey, USA). Temperature (20 °C) and sample flow rate (1.5 standard L min^{-1}) were kept constant in the instrumentation. TDLWintel software provided system control as well as data acquisition and recording at 1 Hz resolution (Daly and Hernandez-Ramirez 2020).

Aerodyne analyzer was coupled with a flow-through, recirculation, non-steady-state chamber. A custom-made cylindrical polyvinyl chloride chamber system consisted of a chamber base and a chamber top. The cross-sectional area of the chamber was 184 cm^2 (15.3 cm diameter). The chamber base was installed 3 cm inside the soil, leaving 7 cm above the soil surface. These chamber bases were installed at the center of each pot at the beginning of the fall phase. The chamber top (5 cm in height) was equipped with two tubing connection ports for gas

196 recirculation (one for inlet and another one for outlet), a stainless capillary tubing (3/16" in inner
197 diameter, 10 cm in length) on the wall for the purpose of pressure equilibration, and rubber seals
198 fitted to the chamber top to ensure headspace closure. The total chamber headspace was 2.2 L.
199 The chamber enclosure and sample recirculation with the Aerodyne lapsed for 3 minutes.

200 During every flux measurement, air temperature and pressure were recorded by a HOBO
201 UX100-001 data logger and a Testo 511 barometer (Testo Inc., Lenzkirch, Germany),
202 respectively.

203 **2.4 Measurements of CO_2 fluxes**

204 During the fall and freezing phases, CO_2 fluxes from the same soil pots were determined by a
205 simple system, which included a Picarro G2508 cavity ring-down spectroscope (CRDS) with a
206 105 mL analytical cell at a constant 140 Torr pressure and at a temperature of 45 °C (Picarro,
207 Santa Clara, CA, USA), a low-leak diaphragm A0702 pump (Picarro, Santa Clara, CA, USA)
208 and the custom-made chamber described above. Similar to the N_2O measurements with the
209 Aerodyne, a vacuum pump enabled the re-circulation of gas sample flow through the chamber
210 headspace at a rate of 240 standard mL min^{-1} during an enclosure time of 3 min.

211 After soil thawing (following Day 56 after the urea addition), CO_2 fluxes were measured
212 with an automated chamber system, which included the CRDS described above, and an eosMX
213 multiplexer connected to 12 eosAC automated chambers (Eosense Inc., Dartmouth, NS, Canada)
214 (Roman-Perez and Hernandez-Ramirez 2021). The total headspace of the automated chamber
215 system was 2.8 L. Each flux measurement lapsed 10 min.

2.5 Flux calculation

The daily fluxes of N_2O and CO_2 were calculated as follows:

$$F = (\frac{dC}{dt}) \times (\frac{V}{S}) \times (\frac{P}{R \times T}) \times M \times k \quad [1]$$

where F is the gaseous flux (μg kg^{-1} d^{-1}), dC/dt is the slope of a simple linear regression or as the first derivative of a quadratic regression at t_0 (μL L^{-1} s^{-1}), V is the headspace volume of the gas chamber (L); S is the dry soil weight (kg), P is the pressure in the chamber headspace during measurement (atm), R is the gas constant (atm μL K^{-1} μmol^{-1}), T is the temperature at chamber headspace during measurement (K), M is the molar mass of N within N_2O (28 g mol^{-1}), or C within CO_2 (12 g mol^{-1}), and k is a conversion factor for the flux unit (from μg kg^{-1} s^{-1} to μg kg^{-1} d^{-1}).

2.6 Calculations of N_2O derived nitrification and denitrification

With the aim of examining the contributions of nitrification and bacterial denitrification processes to the total N_2O production, the N_2O measurements conducted 1 day after thawing were used to estimate the site preference (SP) under natural abundance. This is because the large N_2O production on this day improved the accuracy of isotopic ratio measurements (Waechter et al. 2008).

Calculations for $^{15\alpha}R$, $^{15\beta}R$, $\delta^{15\alpha}N_2O$, $\delta^{15\beta}N_2O$, and $\delta^{15bulk}N_2O$ were as follows:

$$^{15i}R = \frac{^{15i}N}{^{14}N} \ (i = \ \alpha \ or \ \beta) \quad [2]$$

$$\delta^{15i}N_2O = \left(\frac{^{15i}R_{sample}}{^{15}R_{std}} - 1\right) \times 1000 \ (i = \ \alpha \ or \ \beta) \quad [3]$$

$$\delta^{15bulk}N_2O = \frac{\delta^{15\alpha}N + \delta^{15\beta}N}{2} \quad [4]$$

where $^{15\alpha}$N, $^{15\beta}$N and ^{14}N are the mixing ratios of $^{15\alpha}$N-N_2O, $^{15\beta}$N-N_2O and ^{14}N-N_2O in the sample as measured with Aerodyne, respectively; $^{15\alpha}$R is the isotopic ratio of $^{15\alpha}$N to ^{14}N; $^{15\beta}$R is the ratio of $^{15\beta}$N to ^{14}N; $^{15}R_{std}$ is the isotopic ratio in the atmospheric dinitrogen (N_2) ($^{15}R_{std}$ = 0.003676).

The $\delta^{15\alpha}N_2O$ and $\delta^{15\beta}N_2O$ emitted from each experimental pot during chamber enclosure was obtained from the intercept of Keeling plots (i.e., from a linear regression of $\delta^{15\alpha}N_2O$, $\delta^{15\beta}N_2O$, or atom%$^{15}N_2O$ as y-axis vs. 1/total N_2O as x-axis including 180 data points for each chamber measurement of each replicated soil pot separately) (Harris et al. 2017, Thilakarathna and Hernandez-Ramirez 2021).

The intramolecular ^{15}N-N_2O SP was calculated as follows:

$$SP = \delta^{15\alpha}N_2O - \delta^{15\beta}N_2O \quad [5]$$

The isotopic fractionation effect of the transformation from N_2O to N_2 was accounted for based on relationships between $\delta^{15}N_2O$ and SP (Yamamoto et al. 2017, Congreves et al. 2019). The

243 resultant changes in SP magnitude were minor (Daly and Hernandez-Ramirez 2020), extending
244 from negligible to -2.5‰ in only 6% of the individual measurements.

245 The contributions of nitrification and bacterial denitrification to N_2O production were calculated
246 as follows:

$$F_{ni}(\%) = \frac{SP}{33} \times 100 \quad [6]$$

$$F_{deni}(\%) = \frac{33 - SP}{33} \times 100 \quad [7]$$

247 where F_{ni} and F_{deni} are the proportional contributions of nitrification and denitrification,
248 respectively. This assumes that the SPs of the nitrification and denitrification sources are 0 and
249 33 ‰, respectively (Sutka et al. 2006).

250 **2.7 Calculation of the N_2O derived from SOM-N and the priming effects**

251 As our study used urea labelled with ^{15}N, a mass balance based on isotopic composition of
252 the emitted N_2O (atom%) was conducted to separate the contributions of two N pools (i.e., added
253 urea-N vs. existing SOM-N sources) to the overall N_2O flux using the entire dataset over the
254 thawing phase. Atom%$^{15}N_2O$ is the isotopic percentage of ^{15}N in N_2O as follows:

$$Atom\%^{15}N_2O = \frac{\frac{^{15\alpha}N + {}^{15\beta}N}{2}}{^{15\alpha}N + {}^{15\beta}N + {}^{14}N} \times 100 \quad [8]$$

255 Similar as for the SP derivation described above, the atom%$^{15}N_2O$ emitted from each
256 experimental soil pot during each chamber enclosure was obtained from the Keeling plot
257 intercepts.

258 The fractions of N_2O production derived from added ^{15}N-urea and from SOM-N were
259 calculated as follows:

$$FN_2O_{15N-urea}(\%) = \frac{Atom\%^{15}N_2O_{15N-urea} - Atom\%^{15}N_2O_{control}}{5\% - Atom\%^{15}N_2O_{control}} \quad [9]$$

$$FN_2O_{SOM}\ (\%) = \frac{5\% - Atom\%^{15}N_2O_{15N-urea}}{5\% - Atom\%^{15}N_2O_{control}} \quad [10]$$

$$N_2O_{SOM} = FN_2O_{SOM} \times N_2O\ flux\ from\ urea\ ammended\ soil \quad [11]$$

260 where $FN_2O_{15N\text{-}urea}$ and FN_2O_{SOM} are the fractions of N_2O production derived from added ^{15}N-
261 urea and from existing SOM-N, respectively; Atom%$^{15}N_2O_{15N\text{-}urea}$ and Atom%$^{15}N_2O_{control}$ are the
262 isotopic percentages of ^{15}N in N_2O emitted from the experimental pots with and without added
263 urea, respectively; $N_2O_{control}$ is the N_2O flux from the control soils (without urea).

264 The priming effect of daily N_2O fluxes was calculated as follows:

$$N_2O\ priming\ effect = N_2O_{SOM} - N_2O_{control} \quad [12]$$

265 In the Eq. [12], N_2O priming effect >0 corresponds to a positive priming effect caused by
266 added urea, whereas <0 indicates a negative priming effect. More specifically, daily negative

priming was identified when the mean daily SOM-derived N_2O flux from a urea-amended soil was one standard error below the zero baseline (which was defined as the corresponding control without urea addition). Results of N_2O priming were expressed as magnitude and also in relative basis as a percentage of the total flux for each soil pot receiving urea.

Cumulative fluxes of total N_2O and CO_2 as well as urea-derived N_2O, SOM-derived N_2O and primed N_2O after thawing were calculated by linear interpolations of the consecutive daily flux measurements.

2.8 Measurements of soil properties

Soils were air dried and passed through a 2 mm mesh prior to analyses. Soil extractable NH_4^+ and NO_3^- in the filtrate (2M KCl) were determined by using a SmartChem 200 Discrete Wet Chemistry Analyzer (Westco Scientific Instruments, Inc., Brookfield, CT, US) (McKeague 1978, Carter and Gregorich 2007). The soil organic C and total N were determined by a dry combustion method in a Costech Model EA 4010 Elemental analyzer (Costech International Strumatzione, Florence, Italy). The clay, silt and sand percentages were determined by the rate of settling in a solution with a hydrometer (McKeague 1978, Carter and Gregorich 2007). Soil pH was determined in a mixture with a soil-to-water ratio of 1:2 (McKeague 1978, Carter and Gregorich 2007).

With the aim of measuring ^{15}N isotopic composition in the soil at natural abundance (without addition of labelled urea), soil samples were oven-dried at 60 °C and ball-ground to a fine consistency to ensure homogeneity for isotope analysis. The soil $\delta^{15}N$ was determined by using a

Flash 2000 Elemental Analyzer (Thermo Fisher Scientific, Delft, Netherlands) to dry combust the soil sample converting all N to N_2. This analyzer was interfaced online to a Finnigan Delta V Plus isotopic ratio mass spectrometer (Thermo Electron, Bremen, Germany) to detect the ^{15}N isotope composition.

Based on the ^{15}N isotopic compositions of soil N and N_2O emitted from control soils, isotope discrimination (ε) was calculated as follows:

$$\varepsilon\ (‰) = (\frac{^{15}R_{N2O}}{^{15}R_{soilN}} - 1) \times 1000 \qquad [13]$$

where $^{15}R_{N2O}$ is the isotopic ratio of N_2O emitted on Day 57 (1 day after thawing) and $^{15}R_{soilN}$ is the isotopic ratio of soil N. A positive ε implies the enrichment of ^{15}N during the processes of transforming soil N to N_2O emissions; a negative ε implies a depletion of ^{15}N during this conversion from soil N to emitted N_2O. This ε estimation was based on the premise that the transformation from the SOM-N pools into the emitted N_2O pool was unidirectional.

2.9 Statistical analyses

Statistical analyses were performed in R 3.1.3 (R Core Team 2014) at alpha critical value of 0.05. The data were transformed to meet the assumptions of normality and homoscedasticity as necessary. The effects of manure history (CT vs. SW soils), N (urea vs. control) and soil water content (Low, Medium vs. High) treatments on soil NH_4^+, NO_3^-, cumulative N_2O, SOM-derived N_2O and cumulative CO_2 were examined by three-way analysis of variance (ANOVA) for a fixed-effect model with interaction analysis. We run two-way analysis ANOVA for a fixed-

effect model to determine the effects of manure history and water content on primed N_2O and urea-derived N_2O as well as the differences in the contributions of nitrification and denitrification to the N_2O emitted 1 day after thawing. Tukey's Honest Significant Difference (HSD) test was used to compare the difference further in cases where the treatment effects described above were significant.

3. Results

3.1 Daily and cumulative fluxes of total N_2O production

Throughout the fall and freezing phases, N_2O production was relatively low (Fig. 1). Shortly after the urea and water treatments were established at the beginning of the fall phase, the average daily N_2O flux rose up to 0.75 ± 0.20 µg N_2O-N kg^{-1} d^{-1} on Day 3, then dropped to 0.17 ± 0.01 µg N_2O-N kg^{-1} d^{-1} by Day 9, followed by a gradual increase up to 1.23 ± 0.40 µg N_2O-N kg^{-1} d^{-1} on the last day of the fall phase (Fig. 1). During the freezing phase, the average daily N_2O fluxes were consistently low at 0.22 ± 0.02 µg N_2O-N kg^{-1} soil d^{-1} (Fig. 1).

Robust N_2O fluxes occurred after soil thawing (Fig. 1). Overall, daily N_2O fluxes reached a peak of 71.44 ± 7.08 µg N_2O-N kg^{-1} d^{-1} one day after thawing (on Day 57 of the experiment). More specifically, soils under the Low and Medium moisture regimes peaked on Day 57, whereas soils under High moisture showed an even larger peak on Day 58. After that, fluxes quickly declined to 17.66 ± 3.90 µg N_2O-N kg^{-1} d^{-1} 5 days after thawing (Day 61 of the experiment) (Fig. 1).

323 Subsequently, daily N_2O fluxes continued to decrease gradually. The fluxes on the last day of the
324 experiment (Day 86) averaged 0.76 ± 0.18 μg N_2O-N kg^{-1} d^{-1} (Fig. 1).

325 Following thawing, cumulative N_2O emissions were significantly impacted by the history of
326 manure applications (SW > CT), soil water regime (High > Medium > Low) and urea addition
327 (urea-N > control) (Table 2, Fig. 2a).

328 **3.2 N_2O production derived specifically from SOM-N and priming effects**

329 In parallel with the results of total N_2O emissions, the main effects of urea addition, moisture
330 content, and history of manure applications showed separate, significant impact on the
331 cumulative N_2O production derived from SOM during the period after thawing (Table 2, Fig.
332 2a). It is noted that the interactions amongst these three experimental factors were not significant.
333 Irrespective of soil moisture and manure history effects, soils subjected to fall-banded urea were
334 consistently higher in cumulative SOM-derived N_2O emissions after thawing than the control
335 soils by a difference of 24% (305 vs. 245 μg N_2O-N kg^{-1} soil, P= 0.022; Fig. 2a); this
336 substantiates a positive priming effect of SOM that took place following the rapid, wet thawing
337 of the soils. Furthermore, increasing moisture also significantly increased SOM-derived N_2O
338 emissions (Low: 197 μg N_2O-N kg^{-1} soil, Medium: 292, vs. High: 473, P< 0.001). Likewise,
339 having a history of manure application (SW soil) showed to raise the SOM-derived N_2O
340 emissions by 39% above those of the CT soil (374 vs. 268 μg N_2O-N kg^{-1} soil, P= 0.002).
341 Specifically, there was a tendency for the SW soil to have a numerically higher positive priming

342 effect compared with the CT soil in both magnitude (Fig. 2b) and relative (+17 vs. +6% Fig. 2c)
343 basis.

344 Most of the daily N_2O fluxes following soil thawing showed positive priming (Fig. 3). Soils
345 under Low moisture regime showed a peak of primed daily N_2O fluxes 1 day after thawing (Fig.
346 3a). In the case of soils under Medium and High moisture regimes, the peak of positive priming
347 in daily N_2O fluxes occurred 1 day later (i.e., 2 days after thawing) (Fig. 3b and Fig. 3c). Across
348 the three moistures in the SW soil, the peak of daily positive priming was greater at the two
349 higher moisture contents (29.44 μg N_2O-N kg^{-1} d^{-1} at Low vs. 62.95 at Medium and 52.82 at
350 High moisture content). Overall, peak primings were greater for SW than for CT soil under both
351 Medium and High soil moisture regimes (Fig. 3). In general, following these early peaks, primed
352 N_2O fluxes gradually dropped back to approximately the zero baseline.

353 Interestingly, about 2 weeks after soil thawing, negative priming of daily N_2O fluxes was clearly
354 observed (i.e., SOM-derived N_2O << control N_2O). These episodes of evident negative primings
355 occurred only under High soil moisture for both SW and CT soils (Fig. 3c). The negative
356 priming effect began slightly earlier in the SW soil (Day 70 of the experiment) than in the CT
357 soil (Day 71) (Fig. 3c). The last day that registered negative priming effect in SW soil was Day
358 86 of the experiment; in CT soil, it was Day 85. Towards the end of the experiment, the
359 magnitude of the priming effects returned to zero or became minor. Collectively, the results
360 indicate that higher moisture generated more dynamic priming activity.

Contrary to the wide responses of cumulative and daily SOM-derived N_2O fluxes to urea addition, history of manure applications and soil moisture as aforementioned, the direct contribution of the urea-N source to cumulative N_2O fluxes (urea-derived N_2O) was consistent across all assessed experimental factors and treatment combinations, with no significant effects caused by manure history or soil moisture (Table 2, Fig. 2a).

3.3 Contributions of denitrification to the peak of N_2O fluxes

The very large N_2O fluxes that occurred 1 day after soil thawing provided the opportunity to measure and allocate the N_2O produced from nitrification and denitrification sources in all unamended control soils (i.e., under natural ^{15}N abundance conditions) and across the three moisture contents (Fig. 4). The results for ^{15}N-N_2O SP ranged from 1.0 ‰ in the CT soil under High moisture to 5.7 ‰ in the SW soil under Medium moisture (P> 0.05) (Fig. 4c). This suggest that denitrification dominated the vigorous N_2O production, with 83% contribution in the case of the SW soil under Medium moisture and up to nearly all the N_2O produced in the case of the CT soil under High moisture (97%) (Fig. 4b). When averaging across the three moistures, the relative contributions of denitrification to N_2O production in the CT soil were marginal-significantly larger than those in the SW soil (P= 0.06; Fig. 4b).

3.4 Isotopic depletion of ^{15}N-N_2O relative to soil N

There was a consistently negative depletion of ^{15}N (ε) during the transformation from the soil N pool to the emitted N_2O pool across all soil management histories and water regimes (Table 3).

3.5 Inorganic soil N concentrations

There were no significant effects of experimental factors on the NH_4^+ concentrations (Table 2). There was a significant interaction of manure history and water content on soil NO_3^- concentrations (Table 2, Fig. 5). Specifically, irrespective of urea addition, soil NO_3^- concentration was significantly lower in the treatment combination of CT soil at Low moisture than most of other treatments, with the only exception of the treatment combination of CT soil at Medium moisture (data not shown). The NO_3^- concentration apparently increased with increasing soil moisture content in CT soils, but this pattern was not found in SW soils (Fig. 5b). The NO_3^- concentration was in general greater in the SW soil than the CT soil (Fig. 5b). As expected, soils receiving added urea had greater increments in the NO_3^- concentration than the soil without urea (i.e., CT + urea > CT control; SW + urea > SW control, Fig. 5b). These increased nitrate concentrations indicate the occurrence of nitrification in these soils. Furthermore, both NH_4^+ and NO_3^- concentrations increased over time from the beginning to the end of the experiment, including in the control soils; therefore, this indicates that active mineralization and ammonification from SOM-N also took place over the experimental period.

3.6 Soil CO_2 fluxes

Within most of the fall and freezing phases, CO_2 fluxes were generally low and relatively stable across all treatment combinations. Over the fall phase, CO_2 fluxes averaged 1.29 ± 0.13 μg CO_2-C kg^{-1} d^{-1} (Fig. 1c). Afterwards, CO_2 fluxes steadily decreased to 0.57 ± 0.14 μg CO_2-C kg^{-1} d^{-1} on Day 6 of the freezing phase, and then became negligible (Fig. 1c).

Similar to N_2O fluxes, most of the dynamics of CO_2 fluxes took place shortly after soil thawing (Fig. 1). Three days after thawing, the average CO_2 flux across all treatments sharply peaked at 8.65 ± 0.29 μg CO_2-C kg^{-1} d^{-1}. Thereafter, CO_2 fluxes slowly decreased over time, reaching 1.94 ± 0.16 μg CO_2-C kg^{-1} d^{-1} on the last day of the experiment (Fig. 1c). It is noted that there was a strong correlation between daily CO_2 and N_2O fluxes following thawing (r=0.968, P<0.001; Supplementary Fig. 1 and Fig. 1), with the exception of the first 3 days after thawing when the N_2O fluxes were decoupled and disproportionally larger than the measured CO_2 fluxes.

Over the entire experiment and specifically in the period after thawing, the cumulative CO_2 emissions significantly increasing with higher soil moisture in the SW soil that had not received fall-urea (data not shown; Table 2).

4. Discussion

4.1 Added urea triggered primed N_2O emissions derived from SOM-N

Results suggest that fall-applied N fertilizer induces a net positive priming effect from SOM-N at the onset of the subsequent spring thaw. This is consistent with earlier studies showing that fall N applications lead to large thaw-associated N_2O emissions (Burton et al. 2008, Lin et al. 2017). This is the first time in the literature that the direction and magnitude of potential priming effects on augmented N_2O emissions shortly after thawing has been quantified (Fig. 2, Fig. 3). These results suggest that mineralization of SOM increases over a strong freeze-thawing cycle because of the indirect influence of an earlier fall-banded urea, leading to large gaseous N losses at the

419 onset of thawing. Shortly after thawing, the input of extra N substrates from added urea in
420 conjunction with heat and moisture activated microbial activity, collectively accelerating SOM-
421 N availability (Curtin et al. 2012, Curtin et al. 2014). Such additional mineralized SOM-N in the
422 soils amended with urea would become available for nitrifiers and denitrifiers, consequently
423 producing extra SOM-derived N_2O fluxes consistently above the unamended baseline soils.
424 Recent studies have postulated a stoichemetry-based hypothesis with the aim to explain how an
425 addition of labile N (e.g., urea) could prime SOM mineralization (Chen et al. 2014, Roman-Perez
426 and Hernandez-Ramirez 2021). This hypothesis is centered on stoichemetric pre-requirements
427 for SOM decomposition where adding labile N to soils rich in SOM satisfies microbial requisites
428 for undertaking faster decomposition and mineralization of the existing SOM.

429 ### 4.2 Influence of manure history on N_2O emissions derived from SOM-N

430 In addition to the priming of SOM-N caused by labile N additions, soils can be predisposed to
431 exhibiting inherent priming because of the legacy effects from earlier management choices
432 (Ginting et al. 2003, Blagodatskaya et al. 2007, Thilakarathna and Hernandez-Ramirez 2021). It
433 is plausible that the manured soils (SW) in our study showed a more intense response of primed
434 N_2O dynamics to the fall-applied urea because the previous field manure injections in this soil
435 had increased the easily decomposable SOM. It is noted that the SW soil showed a tendency for
436 higher organic C concentrations than CT (Table 1). Conversely, it is acknowledged that
437 increasing SOM concentrations have shown to lead to microbial immobilization of the available
438 N in certain studies (Hou et al. 2000, Zimmerman et al. 2011). Moreover, availability of labile
439 organic C could also reduce the N_2O priming in urea-amended soils. This is explained by the

increased conversion of N_2O into N_2 as driven by heterotrophic utilization of organic C that enhances the last step of bacterial denitrification (Daly and Hernandez-Ramirez 2020). Future research focusing on these drivers of N_2O priming would help to deepen our understanding of C and N turnover in soils, particularly in agricultural systems that experience high, frequent nutrient outputs and inputs such as croplands that receive heavy manure additions. We hypothesize that in environments that are N-rich and even N-saturated, coupling availabilities of C and N could reduce and even cancel the potential priming effects on N_2O emissions derived from SOM-N.

4.3 Moisture regime altered the N_2O produced from SOM-N

In addition to the effects of contrasting manure history on N_2O priming following thawing, soil moisture clearly affected the dynamics of primed N_2O fluxes as well. Although the overall priming was positive across all experimental combinations, only soils under High moisture experienced negative N_2O priming of daily fluxes and also longer-lasting priming effects as noted above (Fig. 3). The temporal shift of daily priming effects from positive to negative and eventually back to zero priming at High moisture could be explained by the mechanism of preferential substrate utilization. The hypothesis of preferential substrate utilization states that when given a variety of nutrient supplies, microorganisms prefer easily available and highly accessible substrates over recalcitrant substrates (Cheng 1999, Cheng and Kuzyakov 2005, Blagodatskaya and Kuzyakov 2008). Within the context of our study, it could be postulated that at the onset of thawing, soil microbes initially utilized the easily available substrates, and then switched to consuming more complex substrates (e.g., wheat straw residues and roots) in

conjunction with any available inorganic N, and eventually started utilizing the recalcitrant SOM. When the soil microbes switch to decomposing plant residues, they would need to uptake inorganic N available from the soil solution because of the high C:N ratios of wheat straw and roots (Gan et al. 2011); this would induce a temporary net N immobilization, which may have generated the temporal negative priming of N_2O production observed in the urea-amended soils under High moisture. It is noted that although all assessed soils could possibly experience this phenomenon, this is particularly crucial in the soils that had received urea because there was more inorganic N available to conduct this temporal immobilization. Additionally, this short-term immobilization could even entail a pool substitution of urea-N in lieu of native inorganic N. These episodes of negative priming could have also become more evident under higher water content because increasing moisture has been found to favor greater SOM-N mineralization and nitrification (Stanford and Epstein 1974, Paul et al. 2003, Curtin et al. 2012, Curtin et al. 2014). The higher N availability with increasing water content is partly shown by the tendency of increased NH_4^+ and NO_3^- concentrations with higher moisture in the CT soils at the end of the experiment (Fig. 5). In other words, with the decrease in the availability of more easily-decomposable substrates, soil microorganisms can progressively utilize recalcitrant SOM to sustain their ongoing metabolism and growth, which subsequently causes additional N mineralization coupled with a gradually-diminishing negative priming of N_2O production, and this can finally shift the soil system to steadily approach neutral priming.

Provided that climate change predictions include higher precipitation over the fall and winter seasons in the North American Plains (Easterling et al. 2017), our study demonstrates the

potential for exacerbated N_2O emissions in the early spring soon after a wet thawing, which was primarily driven by increased N_2O production from SOM in fertilized, near water-saturated soils (Fig. 2a). This interpretation is consistent with previous studies that evaluated the driving effects of increasing moisture on N_2O peak emissions (Hou, A. et al. 2000, Lin and Hernandez-Ramirez 2020, Roman-Perez and Hernandez-Ramirez 2021). Increasing moisture and microbial activity immediately after soil thawing can have led to the depletion of O_2 concentrations in the soil microsites, and hence mediating an increased N_2O production from denitrification (Yanai et al. 2011).

4.4 Main processes producing N_2O shortly after soil thawing

Irrespective of different soil manure history and moisture levels, the consistent negative isotope discrimination (ε) indicated ^{15}N depletion during the transformation of the SOM-N to the major N_2O fluxes just emitted 1 day after thawing (Table 3). This further suggests that the SOM-N pool was the dominant source for substantial N_2O production in our study because several SOM-N transformations in soils such as mineralization, nitrification and denitrification are known to fractionate against the heavier isotope (i.e., ^{15}N), resulting in ^{15}N depletion in the N_2O product compared to the remaining SOM-N substrate (Högberg 1997). However, it is acknowledged that this specific data were available only one time over the experiment while the key processes responsible for N_2O production (nitrification vs. bacterial denitrification) can fluctuate within a few hours or days. If we consider denitrification to be the main source of significant peak N_2O production following the simulation of a strong soil thawing (Fig. 3), abundant soil NO_3^- (and including the intermediate nitrite) pool inexorably played a role as the primary N substrate

503 contributing to the large N_2O emissions instead of NH_4^+ (and the intermediate hydroxylamine
504 substrate). On the other hand, nitrification could become a key source for N_2O emissions in soils
505 under lower water contents or in years when spring thawing is mild (Davidson 1991, Ruser et al.
506 2006).

507 **5. Conclusions**

508 Adding urea asymmetrically increase the primed N_2O emissions specifically derived from SOM-
509 N. Results indicated that annual croplands receiving fall-banded urea followed by a strong
510 freeze-thaw cycle can manifest accelerated SOM transformations that intensify N_2O emissions in
511 the early spring. In addition to these priming effects triggered by the added urea, N_2O production
512 from SOM was further amplified in soils that have had a recent history of manure applications or
513 experienced increasing moisture during spring thawing.

514

6. Acknowledgements

The authors are very thankful for the technical and human support by Leanne Chai, Kurt Forsch, Rebecca Keating, Alan Lee, Jichen Li and Sumeet Kumar Singh.

7. Funding

We would like to acknowledge Canada Foundation for Innovation (John Evans Leadership Fund [32860]), Alberta Livestock and Meat Agency Ltd. (Alberta Agriculture and Forestry – Innovation Program [2016F034R]), and Natural Sciences and Engineering Research Council of Canada (Discovery Grant [2018-05717]) for their financial support of this research.

8. Conflict of interest

The authors declare that they have no conflict of interest.

9. References

Abalos D, Brown SE, Vanderzaag AC, Gordon RJ, Dunfield KE, Wagner-Riddle C (2016) Micrometeorological measurements over 3 years reveal differences in N_2O emissions between annual and perennial crops. Global Change Biol 22(3):1244-1255

Blagodatskaya E, Blagodatsky S, Anderson T, Kuzyakov Y (2007) Priming effects in Chernozem induced by glucose and N in relation to microbial growth strategies. Appl Soil Ecol 37(1-2):95-105

Blagodatskaya E, Kuzyakov Y (2008) Mechanisms of real and apparent priming effects and their dependence on soil microbial biomass and community structure: critical review. Biol Fertility Soils 45(2):115-131

Burton D, Li X, Grant C (2008) Influence of fertilizer nitrogen source and management practice on N_2O emissions from two Black Chernozemic soils. Can J Soil Sci 88(2):219-227

Butterbach-Bahl K, Baggs EM, Dannenmann M, Kiese R, Zechmeister-Boltenstern S (2013) Nitrous oxide emissions from soils: how well do we understand the processes and their controls?. Philosophical transactions of the Royal Society of London Series B, Biological sciences 368(1621):20130122

Carter MR, Gregorich EG (2007) Soil sampling and methods of analysis. CRC Press, Florida

Chai LL, Hernandez-Ramirez G, Dyck M, Pauly D, Kryzanowski L, Middleton A, Powers L, Lohstraeter G, Werk D (2020) Can fertigation reduce nitrous oxide emissions from wheat and canola fields?. Sci Total Environ 745:141014

Chen R, Senbayram M, Blagodatsky S, Myachina O, Dittert K, Lin X, Blagodatskaya E, Kuzyakov Y (2014) Soil C and N availability determine the priming effect: microbial N mining and stoichiometric decomposition theories. Global Change Biol 20(7):2356-2367

Cheng W, Kuzyakov Y (2005) Root effects on decomposition of organic matter. Roots and Soil Management: Interactions Between Roots and Soil.Agronomy Monograph 48:119-143

Cheng W (1999) Rhizosphere feedbacks in elevated CO_2. Tree Physiol 19(4-5):313-320

Congreves KA, Phan T, Farrell RE (2019) A new look at an old concept: using $^{15}N_2O$ isotopomers to understand the relationship between soil moisture and N_2O production pathways. Soil 5(2):265-274

554 Curtin D, Beare MH, Scott CL, Hernandez-Ramirez G, Meenken ED (2014) Mineralization of
555 soil carbon and nitrogen following physical disturbance: a laboratory assessment. Soil Sci Soc
556 Am J 78(3):925-935

557 Curtin D, Beare MH, Hernandez-Ramirez G (2012) Temperature and moisture effects on
558 microbial biomass and soil organic matter mineralization. Soil Sci Soc Am J 76(6):2055-2067

559 Daly EJ, Hernandez-Ramirez G (2020) Sources and priming of soil N_2O and CO_2 production:
560 Nitrogen and simulated exudate additions. Soil Biol Biochem 149:107942

561 Davidson EA (1991) Fluxes of nitrous oxide and nitric oxide from terrestrial ecosystems.
562 Microbial production and consumption of greenhouse gases: methane, nitrogen oxides, and
563 halomethanes.:219-235

564 Easterling DR, Arnold J, Knutson T, Kunkel K, LeGrande A, Leung LR, Vose R, Waliser D,
565 Wehner M (2017) Precipitation change in the United States. In: Wuebbles DJ, Fahey DW,
566 Hibbard KA, Dokken DJ, Stewart BC, and Maycock TK(eds) Climate Science Special Report:
567 Fourth National Climate Assessment, Volume I. U.S. Global Change Research Program,
568 Washington, DC, pp 207-230

569 Gan Y, Liang B, Liu L, Wang X, McDonald C (2011) C: N ratios and carbon distribution profile
570 across rooting zones in oilseed and pulse crops. Crop and Pasture Science 62(6):496-503

571 Ginting D, Kessavalou A, Eghball B, Doran JW (2003) Greenhouse gas emissions and soil
572 indicators four years after manure and compost applications. J Environ Qual 32(1):23-32

573 Goldberg SD, Muhr J, Borken W, Gebauer G (2008) Fluxes of climate-relevant trace gases
574 between a Norway spruce forest soil and atmosphere during repeated freeze–thaw cycles in
575 mesocosms. Journal of Plant Nutrition and Soil Science 171(5):729-739

576 Grant RF, Lin S, Hernandez-Ramirez G (2020) Modelling nitrification inhibitor effects on N_2O
577 emissions after fall-and spring-applied slurry by reducing nitrifier NH_4^+ oxidation rate.
578 Biogeosciences 17(7):2021-2039

579 Harris E, Henne S, Hüglin C, Zellweger C, Tuzson B, Ibraim E, Emmenegger L, Mohn J (2017)
580 Tracking nitrous oxide emission processes at a suburban site with semicontinuous, in situ
581 measurements of isotopic composition. Journal of Geophysical Research: Atmospheres
582 122(3):1850-1870

583 Högberg P (1997) Tansley review no. 95 ^{15}N natural abundance in soil–plant systems. The New
584 Phytologist 137(2):179-203

585 Hou A, Akiyama H, Nakajima Y, Sudo S, Tsuruta H (2000) Effects of urea form and soil
586 moisture on N_2O and NO emissions from Japanese Andosols. Chemosphere-Global Change
587 Science 2(3-4):321-327

588 Hou AX, Chen GX, Wang ZP, Van Cleemput O, Patrick WH (2000) Methane and nitrous oxide
589 emissions from a rice field in relation to soil redox and microbiological processes. Soil Sci Soc
590 Am J 64(6):2180-2186

591 Intergovernmental Panel on Climate Change (2013) Climate Change 2013: The Physical Science
592 Basis. Cambridge University Press, Cambridge and New York

593 Lin S, Hernandez-Ramirez G (2020) Nitrous oxide emissions from manured soils as a function
594 of various nitrification inhibitor rates and soil moisture contents. Sci Total Environ 738:139669

595 Lin S, Hernandez-Ramirez G, Kryzanowski L, Wallace T, Grant R, Degenhardt R, Berger N,
596 Lohstraeter G, Powers L (2017) Timing of Manure Injection and Nitrification Inhibitors Impacts
597 on Nitrous Oxide Emissions and Nitrogen Transformations in a Barley Crop. Soil Sci Soc Am J
598 81(6):1595-1605

599 McKeague JA (1978) Manual on soil sampling and methods of analysis. Canadian Society of
600 Soil Science, Ottawa

601 McKenzie R, Kryzanowski L, Pauly D (2013) Fertilizer Requirements of Irrigated Grain and
602 Oilseed Crops. http://www1.agric.gov.ab.ca/$department/deptdocs.nsf/all/agdex149. Accessed
603 11 December 2017

604 Ostrom PH, DeCamp S, Gandhi H, Haslun J, Ostrom NE (2021) The influence of tillage and
605 fertilizer on the flux and source of nitrous oxide with reference to atmospheric variation using
606 laser spectroscopy. Biogeochemistry:1-17

607 Parry M, Parry ML, Canziani O, Palutikof J, Van der Linden P, Hanson C (2007) Climate
608 change 2007-impacts, adaptation and vulnerability. Cambridge University Press, Cambridge and
609 New York

610 Paul K, Polglase P, O'connell A, Carlyle J, Smethurst P, Khanna P (2003) Defining the relation
611 between soil water content and net nitrogen mineralization. Eur J Soil Sci 54(1):39-48

612 R Core Team (2014) R: A language and environment for statistical computing. http://www.R-
613 project.org/. Accessed 17 March 2015

614 Roman-Perez CC, Hernandez-Ramirez G (2021) Sources and priming of N_2O production across
615 a range of moisture contents in a soil with high organic matter. Journal of Environmental Quality
616 50(1):94-109

617 Ruser R, Flessa H, Russow R, Schmidt G, Buegger F, Munch J (2006) Emission of N_2O, N_2 and
618 CO_2 from soil fertilized with nitrate: effect of compaction, soil moisture and rewetting. Soil Biol
619 Biochem 38(2):263-274

620 Soil Classification Working Group (1998) The Canadian system of soil classification. NRC
621 Research Press, Ottawa

622 Stanford G, Epstein E (1974) Nitrogen Mineralization-Water Relations in Soils 1. Soil Sci Soc
623 Am J 38(1):103-107

624 Sutka RL, Ostrom NE, Ostrom PH, Breznak JA, Gandhi H, Pitt AJ, Li F (2006) Distinguishing
625 nitrous oxide production from nitrification and denitrification on the basis of isotopomer
626 abundances. Appl Environ Microbiol 72(1):638-644

627 Thilakarathna SK, Hernandez-Ramirez G (2021) How does Management Legacy, Nitrogen
628 Addition and Nitrification Inhibition Impact Soil Organic Matter Priming and Nitrous Oxide
629 Production?. Journal of Environmental Quality 20(1):78-93

630 Thilakarathna SK, Hernandez-Ramirez G, Puurveen D, Kryzanowski L, Lohstraeter G, Powers
631 L, Quan N, Tenuta M (2020) Nitrous oxide emissions and nitrogen use efficiency in wheat: N
632 fertilization timing and formulation, soil N, and weather effects. Soil Sci Soc Am J 84(6):1910-
633 1927

634 Toyoda S, Yano M, Nishimura S, Akiyama H, Hayakawa A, Koba K, Sudo S, Yagi K, Makabe
635 A, Tobari Y (2011) Characterization and production and consumption processes of N_2O emitted
636 from temperate agricultural soils determined via isotopomer ratio analysis. Global Biogeochem
637 Cycles 25(2)

638 Toyoda S, Yoshida N (1999) Determination of nitrogen isotopomers of nitrous oxide on a
639 modified isotope ratio mass spectrometer. Anal Chem 71(20):4711-4718

640 Waechter H, Mohn J, Tuzson B, Emmenegger L, Sigrist MW (2008) Determination of N_2O
641 isotopomers with quantum cascade laser based absorption spectroscopy. Optics Express
642 16(12):9239-9244

643 Wagner-Riddle C, Furon A, Mclaughlin NL, Lee I, Barbeau J, Jayasundara S, Parkin G, Von
644 Bertoldi P, Warland J (2007) Intensive measurement of nitrous oxide emissions from a corn–

645 soybean–wheat rotation under two contrasting management systems over 5 years. Global Change
646 Biol 13(8):1722-1736

647 Wolf B, Zheng X, Brüggemann N, Chen W, Dannenmann M, Han X, Sutton MA, Wu H, Yao Z,
648 Butterbach-Bahl K (2010) Grazing-induced reduction of natural nitrous oxide release from
649 continental steppe. Nature 464(7290):881-884

650 Wu X, Brüggemann N, Gasche R, Shen Z, Wolf B, Butterbach-Bahl K (2010) Environmental
651 controls over soil-atmosphere exchange of N_2O, NO, and CO_2 in a temperate Norway spruce
652 forest. Global Biogeochem Cycles 24(2)

653 Yamamoto A, Akiyama H, Nakajima Y, Hoshino YT (2017) Estimate of bacterial and fungal
654 N_2O production processes after crop residue input and fertilizer application to an agricultural
655 field by ^{15}N isotopomer analysis. Soil Biol Biochem 108:9-16

656 Yanai Y, Hirota T, Iwata Y, Nemoto M, Nagata O, Koga N (2011) Accumulation of nitrous
657 oxide and depletion of oxygen in seasonally frozen soils in northern Japan–Snow cover
658 manipulation experiments. Soil Biol Biochem 43(9):1779-1786

659 Zimmerman AR, Gao B, Ahn M (2011) Positive and negative carbon mineralization priming
660 effects among a variety of biochar-amended soils. Soil Biol Biochem 43(6):1169-1179

661

Tables

Table 1. Soil physical and chemical properties at the 0-15 cm depth increment of the soils with (SW) and without (CT) history of liquid manure injections. Note that only organic carbon showed a magnitude difference between these two soil managements, with SW slightly higher than CT (P > 0.05).

Soil properties		
Classification†	Black Chernozem	
Bulk density (g cm^{-3})	1.11 ± 0.06	
pH	6.1 ± 0.2	
Texture	Clay	
Clay(%)	47.0 ± 1.2	
Silt(%)	36.0 ± 0.3	
Sand(%)	17.0 ± 1.0	
	SW	CT
Organic C (g C kg^{-1})	63.7 ± 5.0‡	61.6 ± 4.3
Total N (g N kg^{-1})	5.9 ± 0.3	5.9 ± 0.4

†Based on the Canadian System of Soil Classification (Soil Classification Working Group 1998).

‡Standard error of the mean.

Table 2. P-values of ANOVA models for soil NH_4^+ and NO_3^- concentrations as well as cumulative N_2O and CO_2 emissions after thawing (Days 56 − 86).

Experimental factor	NH_4^+	NO_3^-	Cumulative N_2O	SOM-derived N_2O	Urea-derived N_2O	Primed N_2O	Cumulative CO_2
History of manure application (Soil)†	n.s.	0.002	0.006	0.002	n.s.	n.s.	n.s.
Water content (Water)‡	n.s.	0.035	<0.001	<0.001	n.s.	n.s.	<0.001
Nitrogen addition (Nitrogen)§	n.s.	<0.001	<0.001	0.022	N/A	N/A	n.s.
Soil × Water	n.s.	0.042	n.s.	n.s.	n.s.	n.s.	n.s.
Soil × Nitrogen	n.s.	n.s.	n.s.	n.s.	N/A	N/A	n.s.
Water × Nitrogen	n.s.	n.s.	n.s.	n.s.	N/A	N/A	n.s.
Soil × Water × Nitrogen	n.s.	n.s.	n.s.	n.s.	N/A	N/A	n.s.

† History of manure application factor included two levels: soils with spring manure (SW) and without a history of liquid manure injections (field control, CT).

‡ Water content factor included three levels: Low, Medium, and High water contents.

§ Nitrogen factor included two levels: with and without urea additions. Soils without urea are also referred as controls.

678 **Table 3. The ^{15}N isotope discrimination [ε, mean ± SE (‰), n= 3] of soil N_2O emitted 1 day**
679 **after thawing (the time of peak emissions in the study) relative to the soil N pool in both**
680 **field control (CT) and manure-treated (SW) soils at various water contents. Calculation**
681 **based on Eq. [13].**

Soil	Water content	Soil × Water Content			Soil		
CT	Low	-10.19	±	11.21	-11.73	±	3.86
	Medium	-7.68	±	2.76			
	High	-17.34	±	4.46			
SW	Low	-18.78	±	3.60	-15.26	±	2.30
	Medium	-15.45	±	4.94			
	High	-11.56	±	3.65			

682

683

Figures

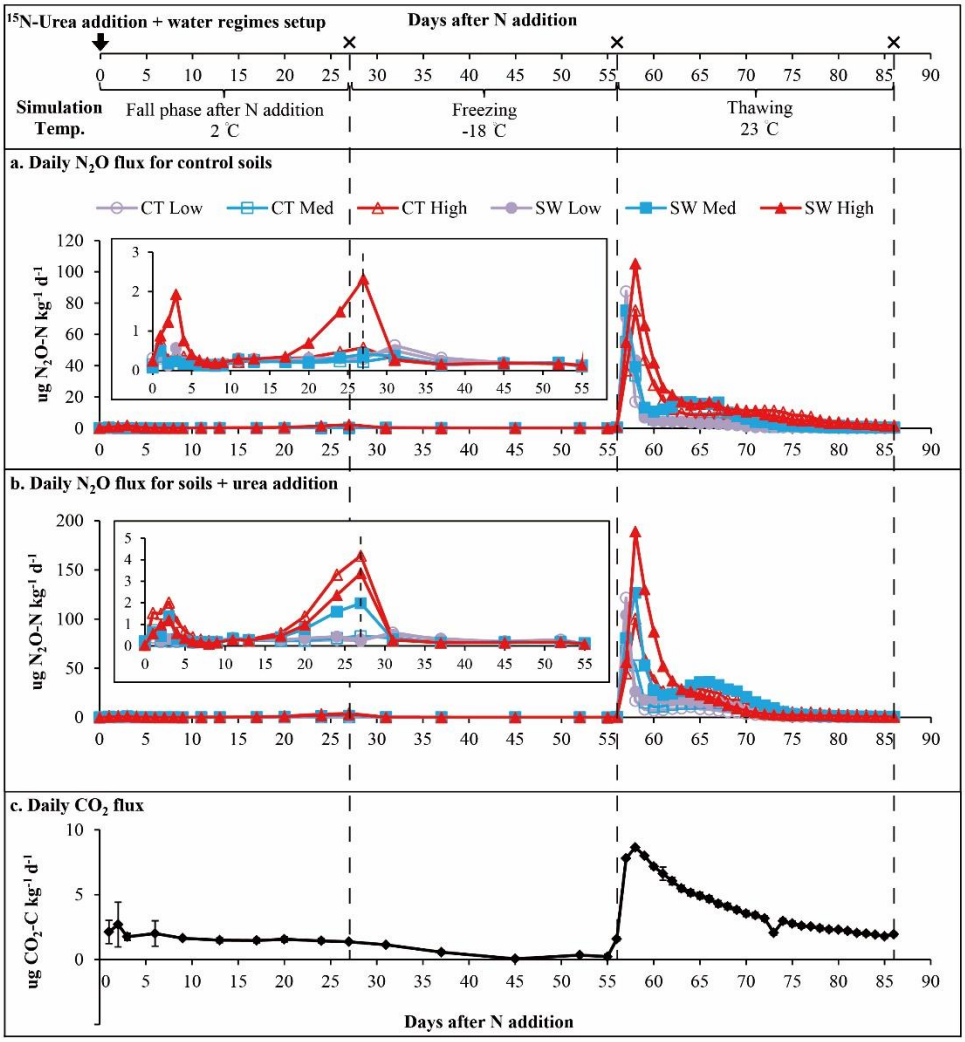

Fig. 1. Daily nitrous oxide (N_2O) and carbon dioxide (CO_2) fluxes from soils over the entire experiment. In the case of N_2O, fluxes are shown in two separate panels as subsets (a) without and (b) with added urea. Fluxes of CO_2 are averaged across all treatment combinations. SW and CT stand for soils with and without a history of manure additions,

respectively. Low, Med, and High correspond to moisture regimes where Med stands for Medium. Error bars correspond to one standard error of the mean.

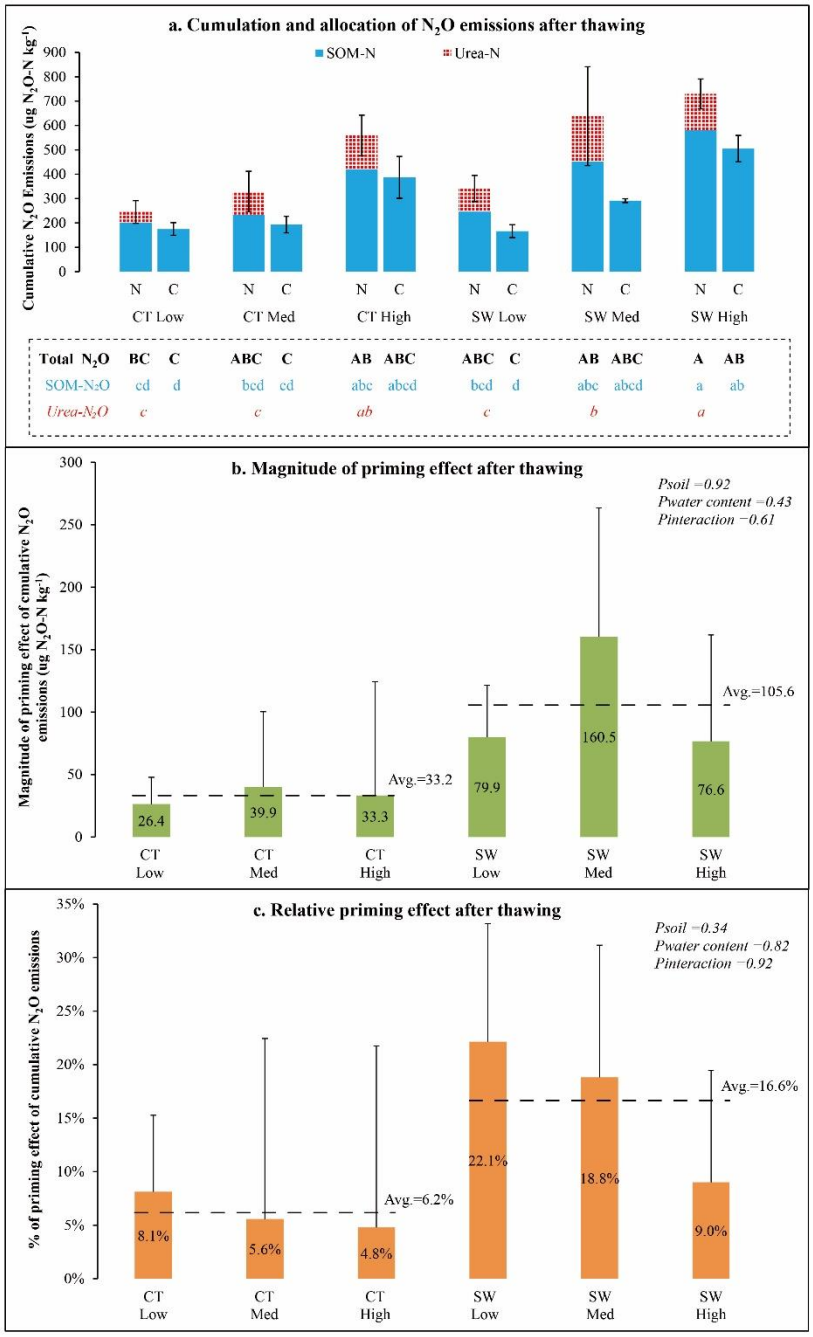

Fig. 2. (a) Cumulative N_2O emissions allocated to urea and soil organic matter (SOM) sources, (b) magnitude priming and (c) relative priming caused by urea addition following soil thawing. SW and CT stand for soils with and without a history of manure additions,

respectively. Low, Med, and High correspond to moisture regimes where Med stands for Medium. In Panel a, N and C acronyms correspond to the urea-N addition treatment and the zero-N addition (control) treatment, respectively. In Panel a, different letters indicate significant difference in total cumulative N_2O (uppercase), SOM-derived N_2O (lowercase) and urea-derived (italic) N_2O emissions after thawing ($P < 0.05$). In Panels b and c, N_2O primings were respectively shown as magnitudes and also in relative basis as percentages of the total fluxes (shown in Panel a) of soil pots receiving urea. Error bars correspond to one standard error.

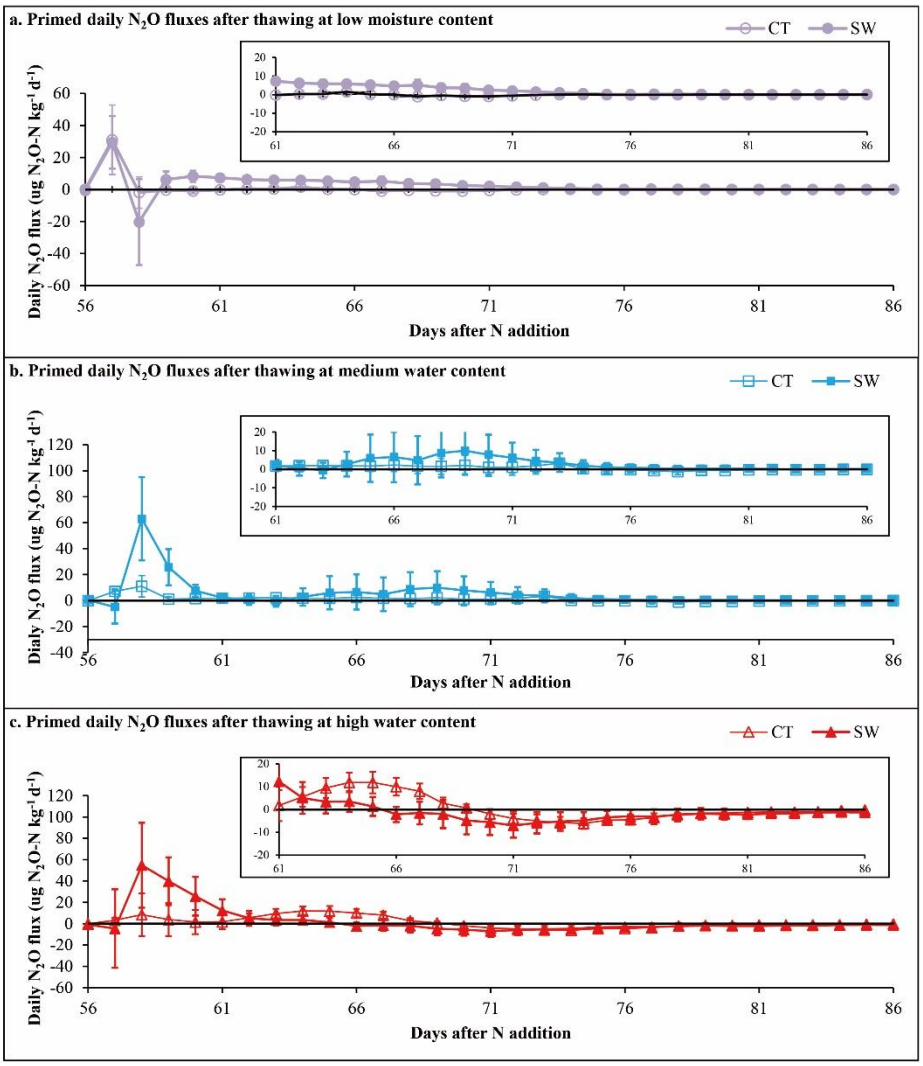

Fig. 3. Primed daily N_2O fluxes following soil thawing. SW and CT stand for soils with and without a history of manure additions, respectively. Low, Med, and High correspond to moisture regimes where Med stands for Medium. Positive and negative primed daily N_2O fluxes represent positive and negative priming effects, respectively. Error bars correspond to one standard error of the mean.

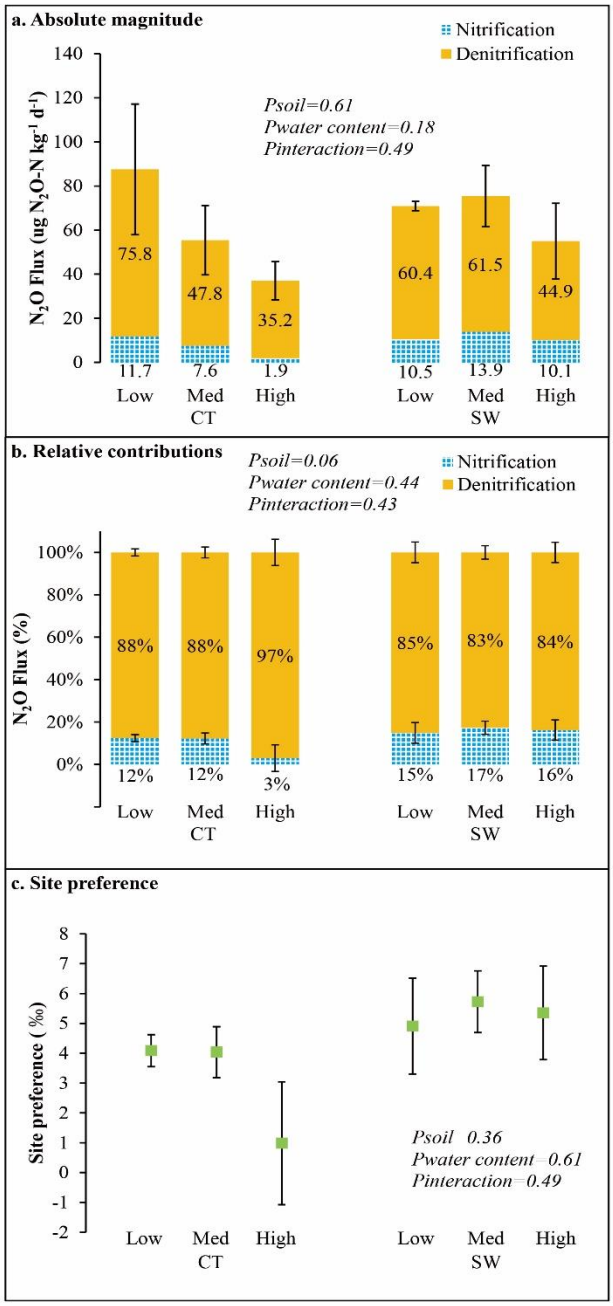

Fig. 4. (a) Magnitude and (b) relative contributions of nitrification and denitrification, as well as (c) site preference for the N_2O fluxes emitted 1 day after thawing (Day 57 of the

experiment). SW and CT stand for soils with and without a history of manure additions, respectively. Low, Med, and High correspond to moisture regimes where Med stands for Medium. In Panels a and b, numbers in the columns are respectively the flux magnitude and percentage of N_2O emissions produced via denitrification or nitrification. Error bars correspond to standard error of the mean.

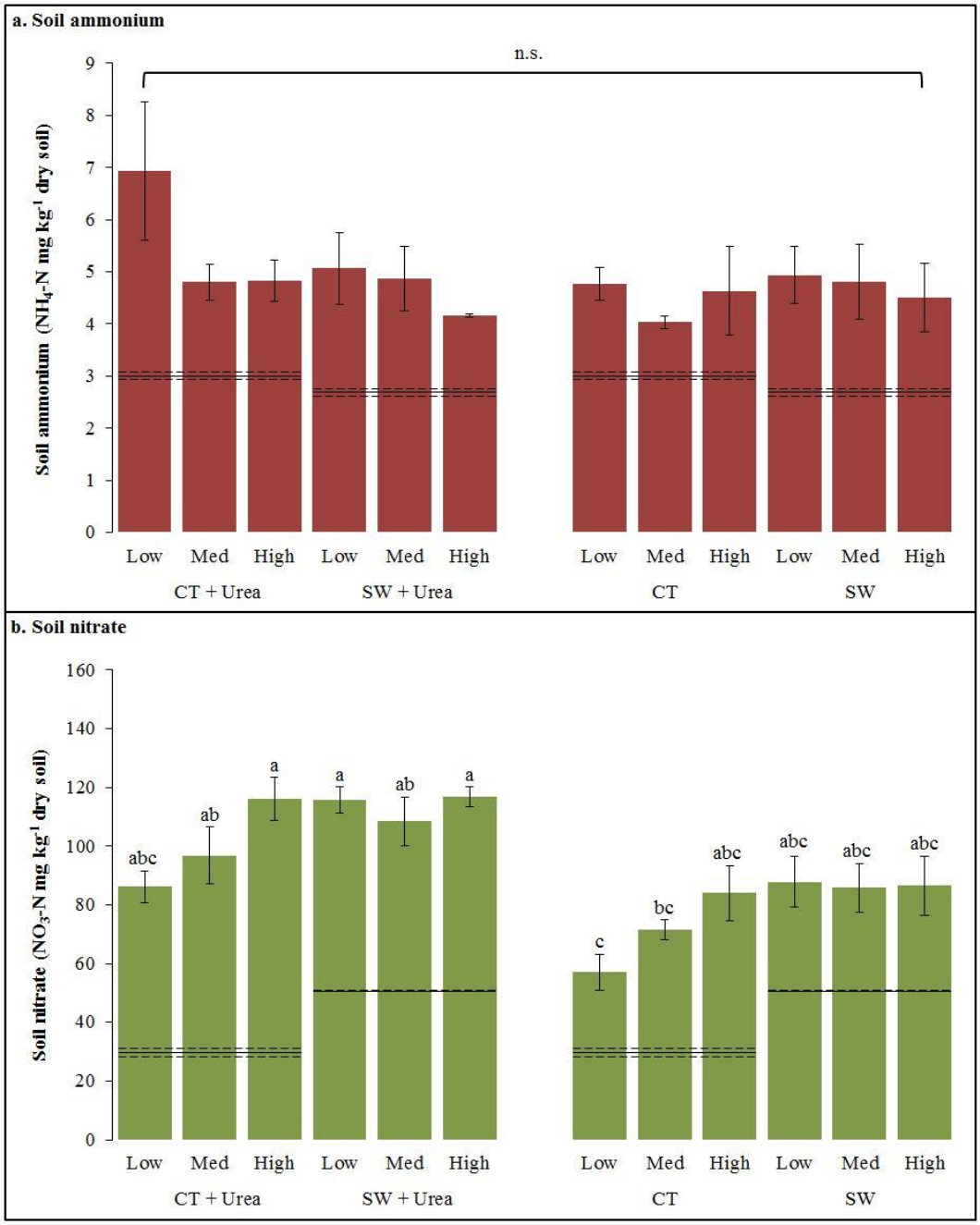

Fig. 5. Soil (a) ammonium and (b) nitrate concentrations at the end of the experiment for the soils with (SW) and without (CT) history of manure additions at Low, Medium (Med) and High moisture regimes. Horizontal lines (with one standard error) across moisture

contents are the concentrations of (a) ammonium and (b) nitrate of the two soils at the beginning of the experiment (prior to urea addition and establishment of the three moisture regimes). Different letters indicate significant differences among treatment combinations ($P < 0.05$). Error bars correspond to one standard error of the mean. n.s. = not significant.

Figures

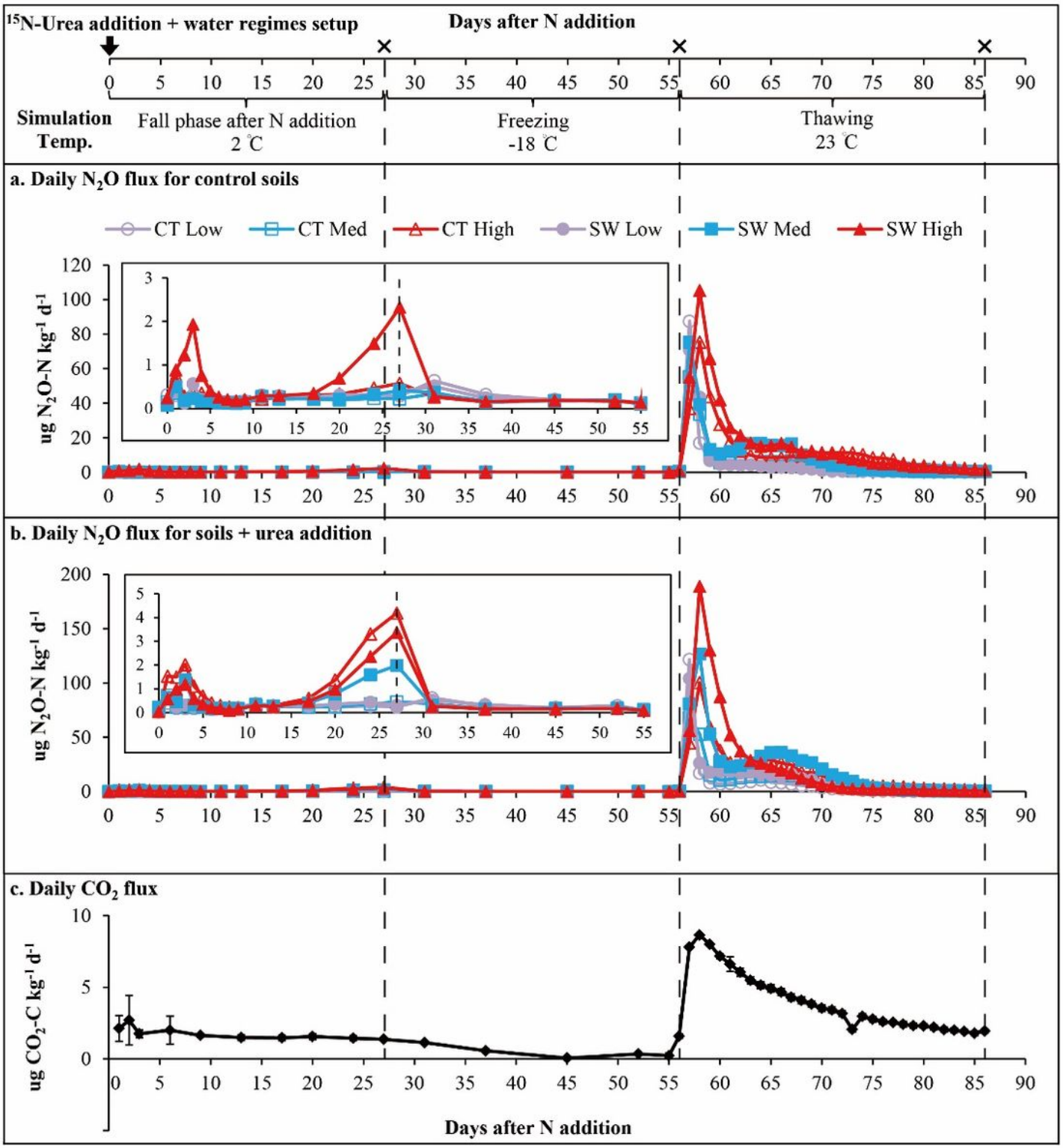

Figure 1

Daily nitrous oxide (N2O) and carbon dioxide (CO2) fluxes from soils over the entire experiment. In the case of N2O, fluxes are shown in two separate panels as subsets (a) without and (b) with added urea. Fluxes of CO2 are averaged across all treatment combinations. SW and CT stand for soils with and

without a history of manure additions, respectively. Low, Med, and High correspond to moisture regimes where Med stands for Medium. Error bars correspond to one standard error of the mean.

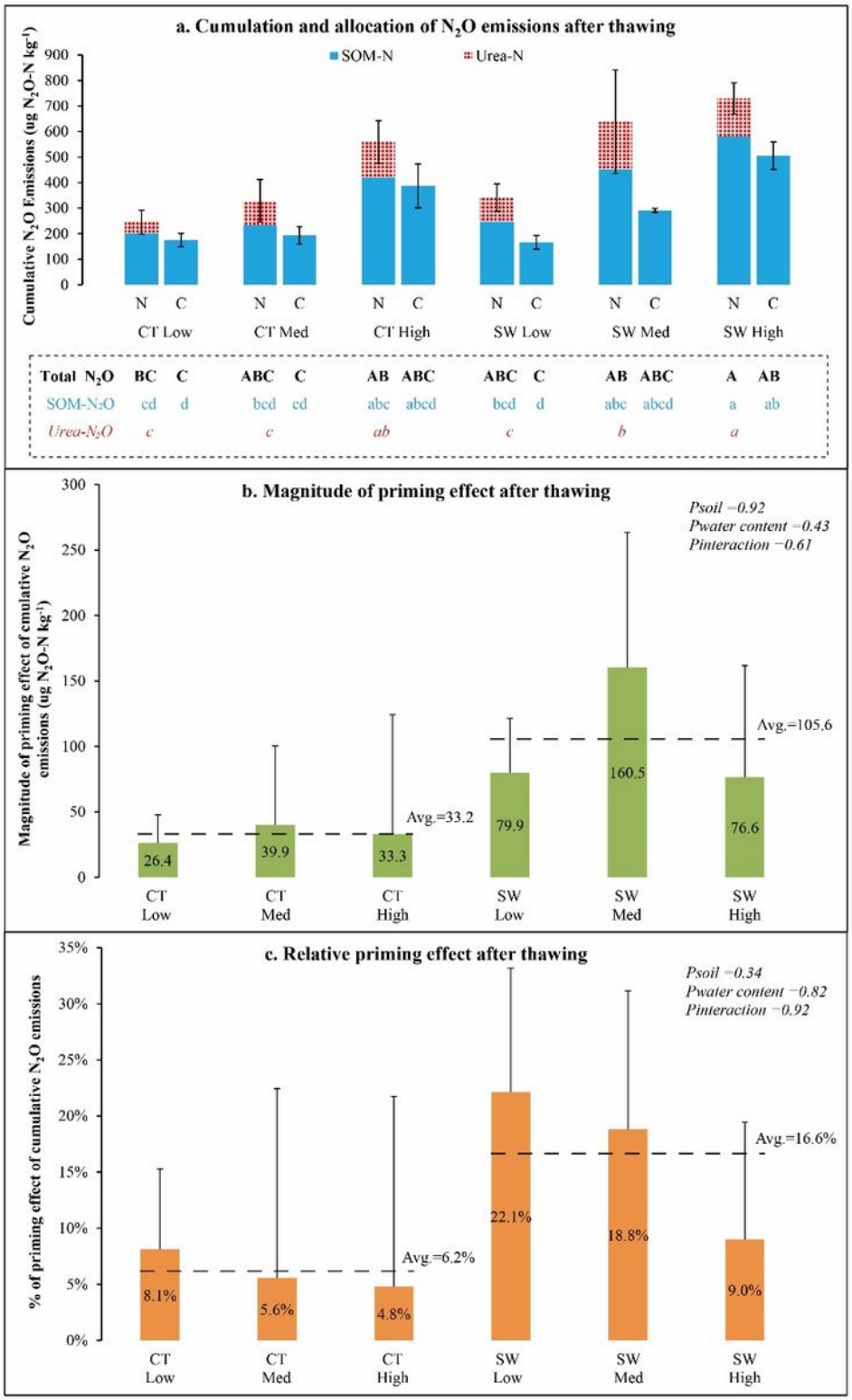

Figure 2

(a) Cumulative N2O emissions allocated to urea and soil organic matter (SOM) sources, (b) magnitude priming and (c) relative priming caused by urea addition following soil thawing. SW and CT stand for soils with and without a history of manure additions, respectively. Low, Med, and High correspond to

moisture regimes where Med stands for Medium. In Panel a, N and C acronyms correspond to the urea-N addition treatment and the zero-N addition (control) treatment, respectively. In Panel a, different letters indicate significant difference in total cumulative N2O (uppercase), SOM-derived N2O (lowercase) and urea-derived (italic) N2O emissions after thawing ($P < 0.05$). In Panels b and c, N2O primings were respectively shown as magnitudes and also in relative basis as percentages of the total fluxes (shown in Panel a) of soil pots receiving urea. Error bars correspond to one standard error.

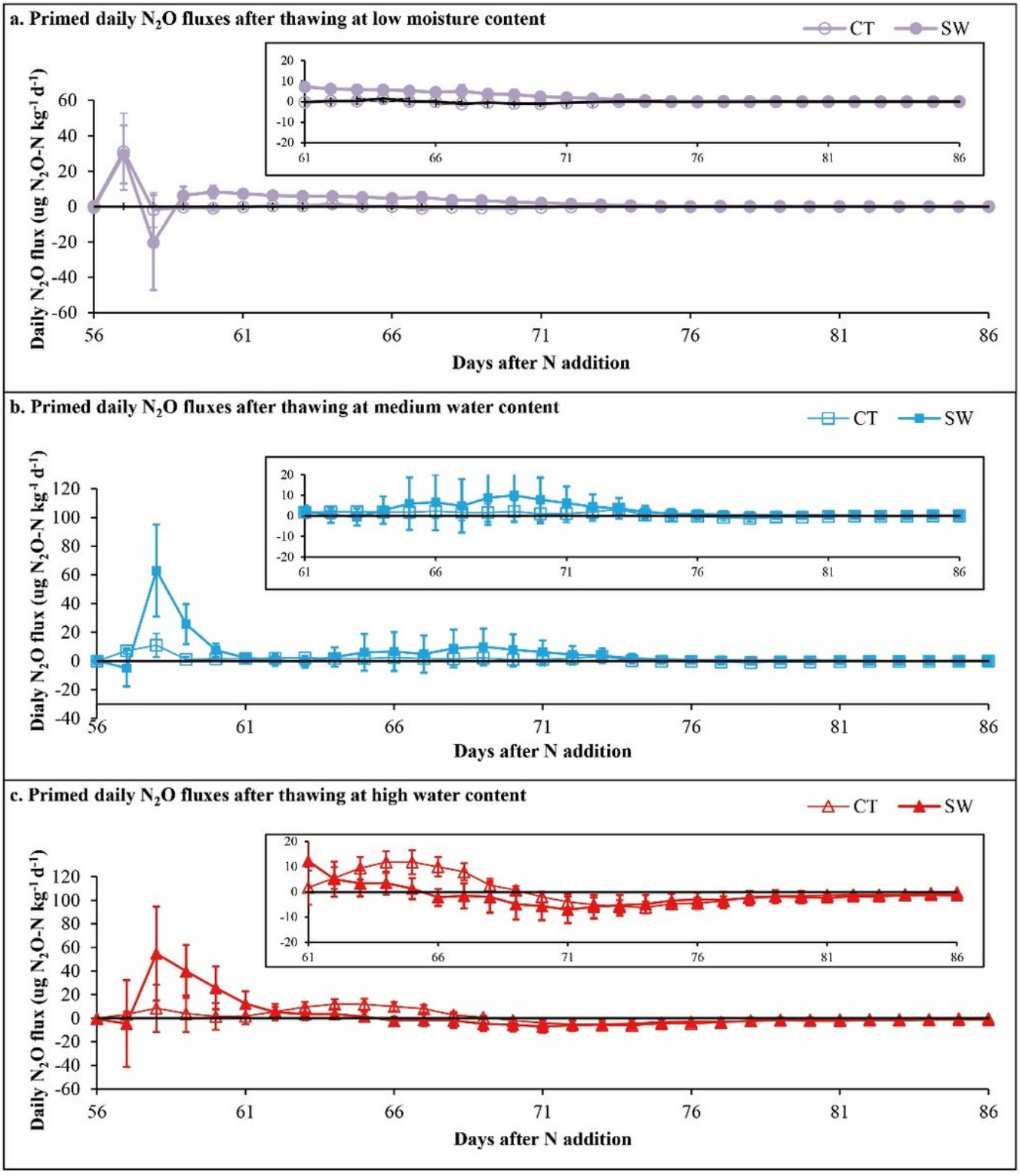

Figure 3

Primed daily N2O fluxes following soil thawing. SW and CT stand for soils with and without a history of manure additions, respectively. Low, Med, and High correspond to moisture regimes where Med stands for Medium. Positive and negative primed daily N2O fluxes represent positive and negative priming effects, respectively. Error bars correspond to one standard error of the mean.

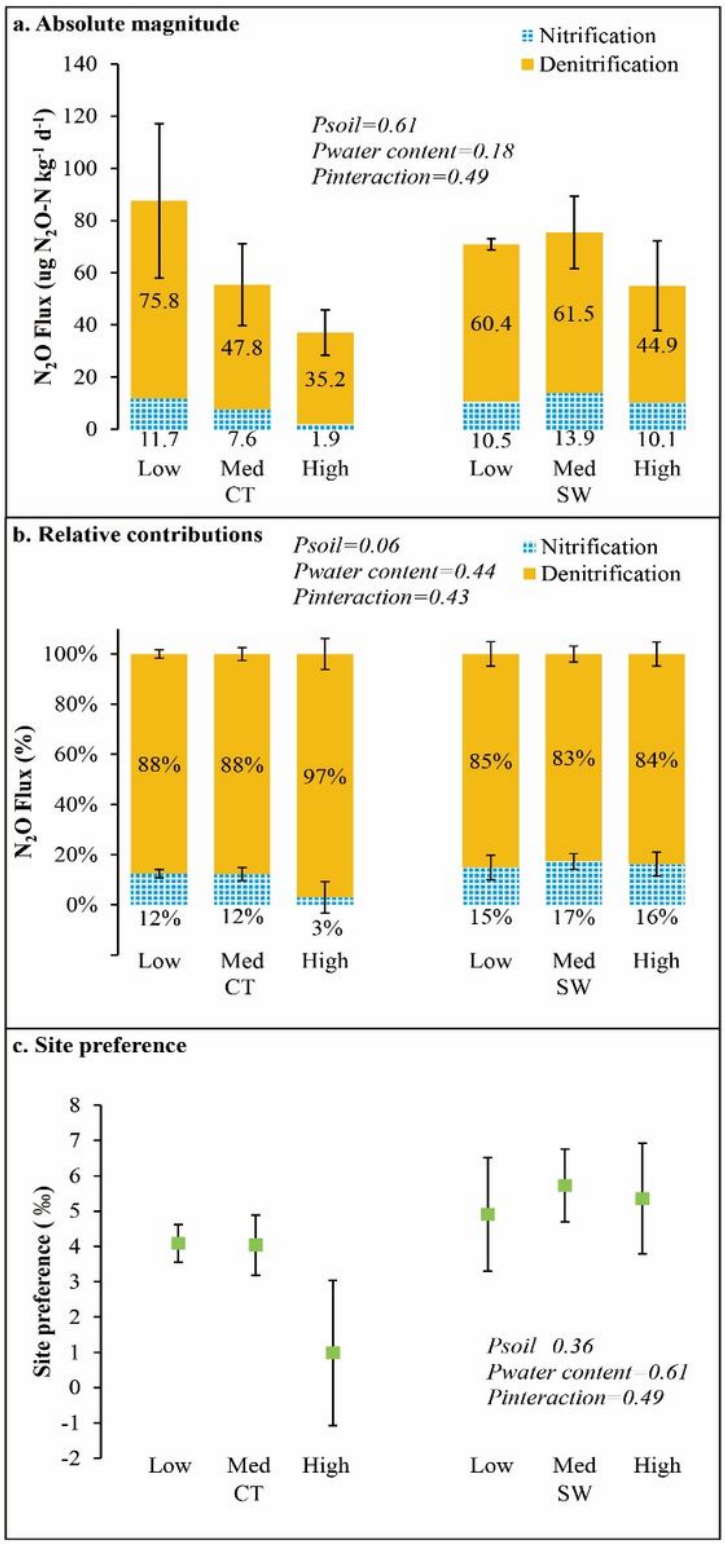

Figure 4

(a) Magnitude and (b) relative contributions of nitrification and denitrification, as well as (c) site preference for the N2O fluxes emitted 1 day after thawing (Day 57 of the experiment). SW and CT stand for soils with and without a history of manure additions, respectively. Low, Med, and High correspond to moisture regimes where Med stands for Medium. In Panels a and b, numbers in the columns are respectively the flux magnitude and percentage of N2O emissions produced via denitrification or nitrification. Error bars correspond to standard error of the mean.

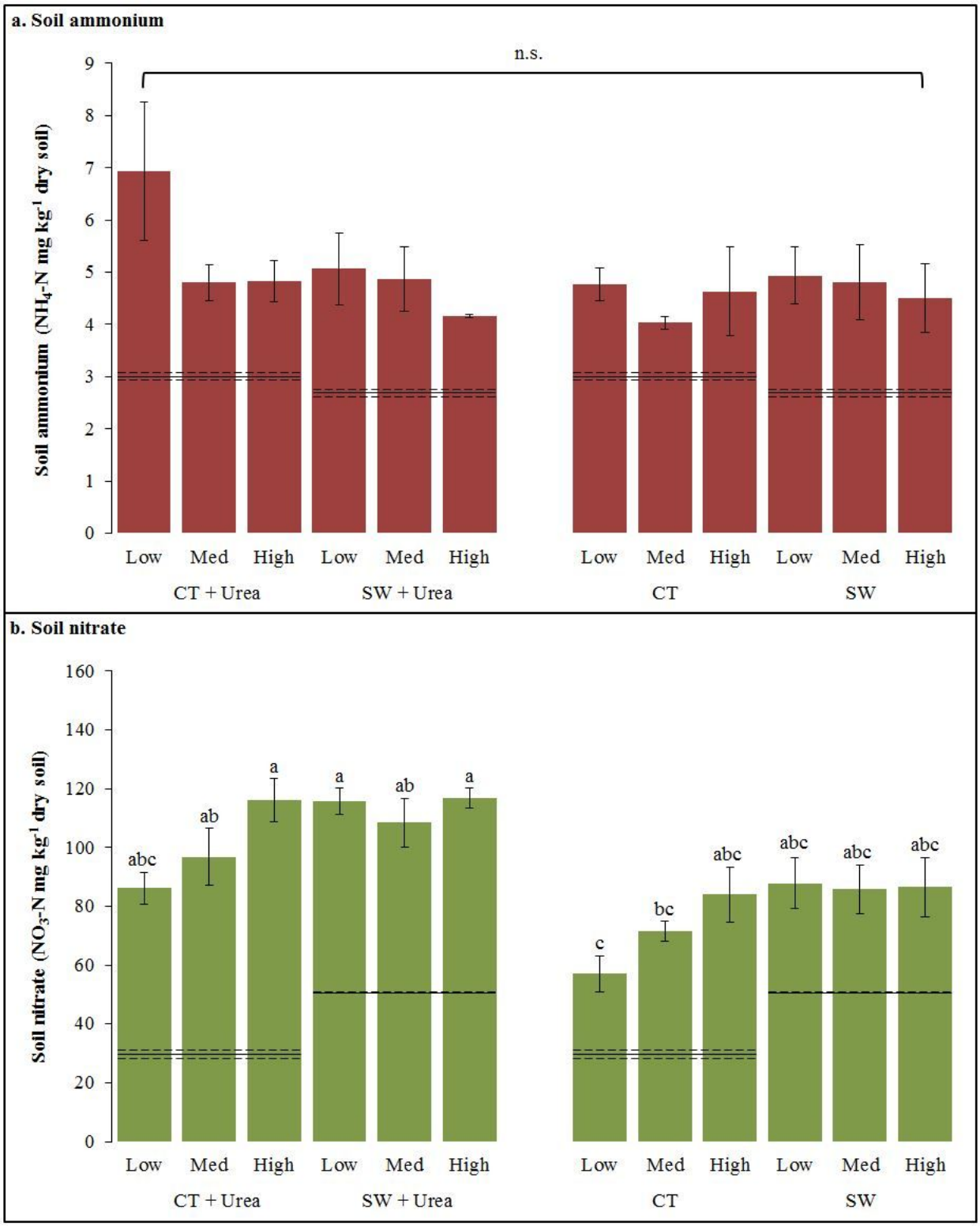

Figure 5

Soil (a) ammonium and (b) nitrate concentrations at the end of the experiment for the soils with (SW) and without (CT) history of manure additions at Low, Medium (Med) and High moisture regimes. Horizontal lines (with one standard error) across moisture contents are the concentrations of (a) ammonium and (b) nitrate of the two soils at the beginning of the experiment (prior to urea addition and establishment of the three moisture regimes). Different letters indicate significant differences among treatment combinations ($P < 0.05$). Error bars correspond to one standard error of the mean. n.s. = not significant.

Supplementary Files

This is a list of supplementary files associated with this preprint. Click to download.

- SupplementarydatamesocosmwoCopyghr.docx